Geology

Unfolding: An inverse approach to fold kinematics

Jaume Vergés, Douglas W. Burbank and Andrew Meigs

Geology 1996;24;175-178
doi: 10.1130/0091-7613(1996)024<0175:UAIATF>2.3.CO;2

Unfolding: An inverse approach to fold kinematics

Jaume Vergés Departament de Geologia Dinàmica, Geofísica i Paleontologia, Universidad de Barcelona, 08071 Barcelona, Spain
Douglas W. Burbank
Andrew Meigs Department of Geological Sciences, University of Southern California, Los Angeles, California 90089

ABSTRACT

Preserved fold shapes usually reveal little about their kinematic evolution. Syntectonic strata preserved in growth synclines in contact with a fold, however, can permit "unfolding": a sequential reconstruction of fold growth backward through time from a geometry observed at present to an initial undeformed state. Such reconstructions can define the kinematics of fold growth. Growth strata associated with anticlinal forelimbs in the Ebro basin exhibit depositional tapering of beds on fold flanks and progressive limb rotation. Unfolding a well-dated detachment fold defines its kinematic evolution and coevally varying rates of shortening, forelimb uplift, and forelimb rotation. Interplay of these rates with sedimentation rates controls onlap and offlap relations.

INTRODUCTION

Folds are a fundamental structure of contractional orogens, and yet deciphering their kinematic history continues to be controversial. Given a present-day cross section of a fold, we are usually unable to determine unambiguously the history of fold growth. Fold geometries from some thrust belts are consistent with geometrically based kinematic models, often with self-similar growth patterns (Medwedeff, 1992; Shaw and Suppe, 1994). Other studies suggest that preserved fold shapes represent only the end product of a geometrically variable growth history (e.g., Ramsay, 1974). The crux of the problem rests in the motion of rocks with respect to fold hinges and the angles of fold limbs with time. Two different data sets can potentially resolve fold evolution: distribution of strain throughout the fold (Fischer et al., 1992) and growth strata (Suppe et al., 1992). Growth strata deposited above the limb of a deforming fold can place clear geometric constraints on fold growth through time. Herein we describe a methodology for a step-by-step restoration of growth strata backward through time (termed "unfolding") to determine fold kinematics. Although our examples formed above detachment folds, the methodology is independent of fold history and should be applicable to other folding styles.

DETACHMENT FOLDS AND RELATED GROWTH STRATA

Along the margins of the Ebro foreland basin (Fig. 1), well-preserved growth strata are associated with numerous folds (Riba, 1976), some of which can be defined as detachment folds (Fig. 2). In our usage, a detachment fold is one that forms by buckling above a detachment which is subparallel to original layering and in which the majority of shortening is accommodated by folding, rather than faulting (Jamison, 1987). The Spanish examples display four salient characteristics when seen in profile (Fig. 1): (1) the full succession of growth strata displays a wedge-shaped geometry; (2) single beds or groups of beds within the wedge-shaped domain thicken across the forelimb from the anticlinal crest to a maximum thickness near the synclinal axis; (3) angular unconformities may occur between groups of beds in the wedge-shaped domain; and (4) growth strata above the forelimb show an increase in dip from stratigraphically higher to lower strata. Whereas the relations described below apply equally well to backlimbs and forelimbs, our discussion is restricted to forelimbs, where angular stratal geometries tend to be more pronounced.

A well-exposed example of the interrelations between syntectonic deposition and evolving structures occurs at Oliana along the eastern oblique margin of the South Central Unit (Fig. 1, A and B). Here, between ~37.2 and 34.0 Ma, an imbricate system of southeast-directed thrusts developed on the backlimb of the Oliana anticline coevally with deposition of growth strata (Vergés and Muñoz, 1990; Burbank et al., 1992). The fold and thrust system is detached above a decollement in Upper Triassic evaporites (Vergés, 1993). Folds in both pregrowth and growth strata show kink-shaped geometries with rounded hinges and interlimb angles ranging from 40° to 70°. We focus on strata preserved in a growth syncline attached to the Can Juncas anticline, which has an overturned forelimb and a wavelength of ~0.5 km (Figs. 1B and 3). Given the typical structural styles of the folds and faults above evaporites in the southern Pyrenees and the absence of surface faults at Can Juncas, we interpret this fold as a detachment anticline.

A pronounced unconformity marks the contact between the base of the growth strata and the overturned pregrowth strata in the fold's forelimb. The oldest growth strata prominently onlap paleotopography that existed prior to fold growth. Clear onlap of the forelimb persisted as folding initiated. From the synclinal axial surface to the crest of the anticline, growth strata show a general thinning defined by marked changes in dip of both individual beds and stratal units (Fig. 4A). These strata comprise 170 m of fluvial deposits characterized by siltstone and sandstone interbedded with conglomerate beds up to 25 m thick. Paleocurrent indicators define flow parallel to the fold crest and synclinal axis.

Few successions of growth strata have been dated with precision sufficient to define short-term variability in rates of sedimentation, uplift, shortening, or forelimb rotation. Paleomagnetic dates on the growth strata of the Can Juncas anticline (Burbank and Vergés, 1994), however, provide ages for three horizons from which rates of sediment accumulation and fold growth can be calculated.

UNFOLDING: REVERSE STEP-BY-STEP FOLD RESTORATION

The methodology relies on a step-by-step unfolding of stratal units backward through time. For each time step, younger growth strata are removed, the uppermost depositional surface or bounding unconformity is restored to its original prefolding orientation, and underlying growth and pregrowth strata are concurrently back rotated. In these fluvial strata, where paleoflow is parallel to the anticlinal trend, a horizontal depositional surface in cross section can be assumed. Transverse rivers or alluvial fans may have slopes of a few degrees. If known, such slopes can be integrated into the restoration.

A deformed-state cross section, parallel to the tectonic transport, at Can Juncas (Oliana) has been built using dip data, map distribution, measured stratigraphic sections, and lengths of tapered and untapered syntectonic strata across the anticline-growth syncline pair (Fig. 4A). Restorations for two stages (35.37 and 34.96 Ma) have been made by pinning the unthinned growth strata in the distal part of the growth syncline well beyond the folded domain, preserving stratal areas, and minimizing changes in taper in order to minimize bed-length changes during folding (Fig. 4, B and C).

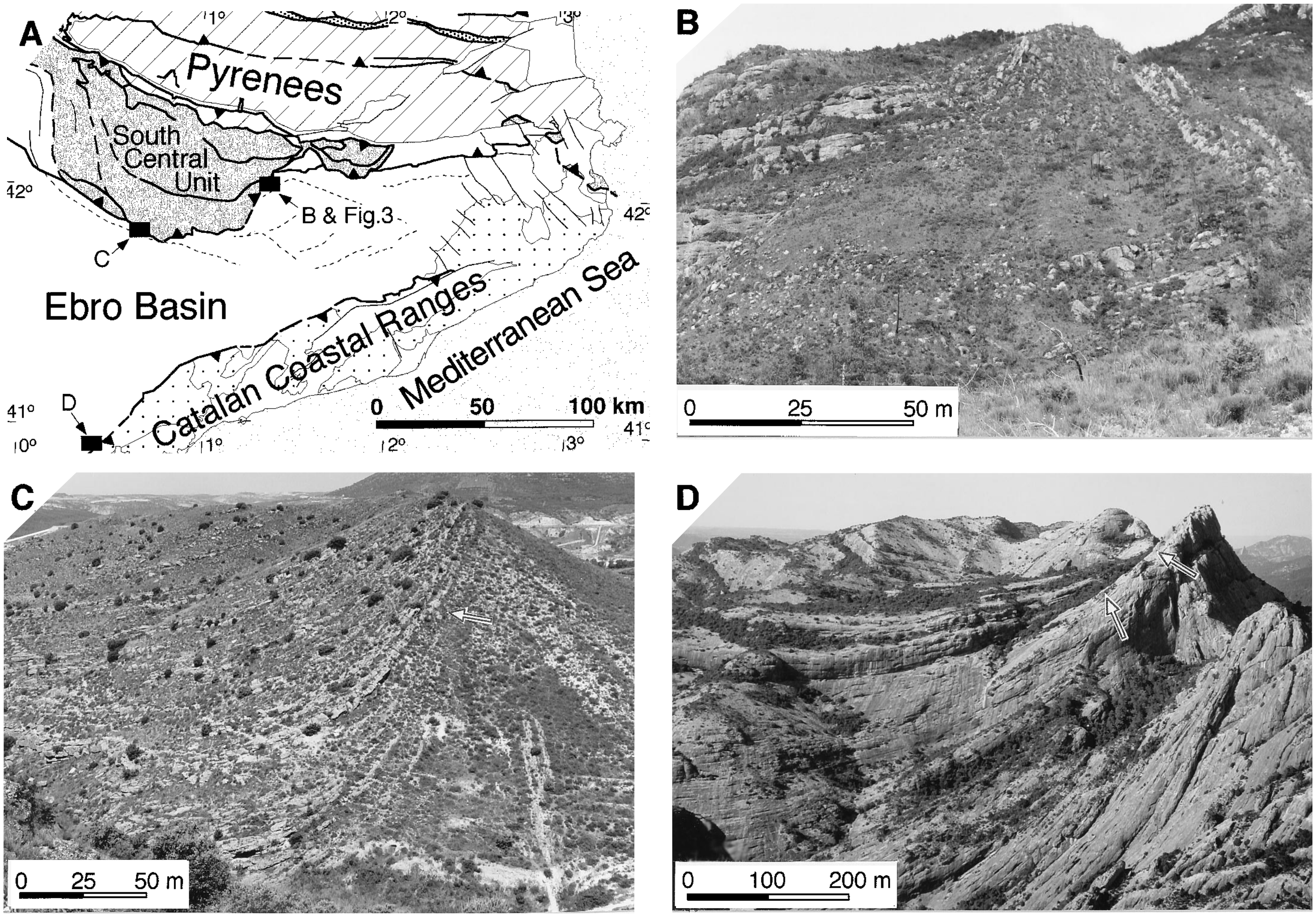

Figure 1. A: Geologic map of Ebro basin with locations of field examples. B: Growth fold at Can Juncas showing prominent thinning toward anticlinal crest in pregrowth strata (top right). C: Internal geometry of evaporite-cored La Garriga fold is dominated by clear onlap of overturned fold forelimb (arrows). D: Growth syncline near Horta de Sant Joan (Barranco dels Estrets) in Catalan Coastal Ranges showing overturned basal conglomerates (at right) deposited on deformed carbonate and siltstone. Note prominent internal unconformity that younger growth strata progressively onlaps (arrows).

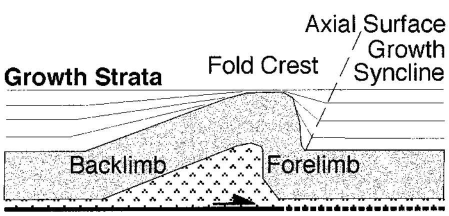

Figure 2. Detachment fold geometry and thickness variations in growth syncline as related to its forelimb and backlimb.

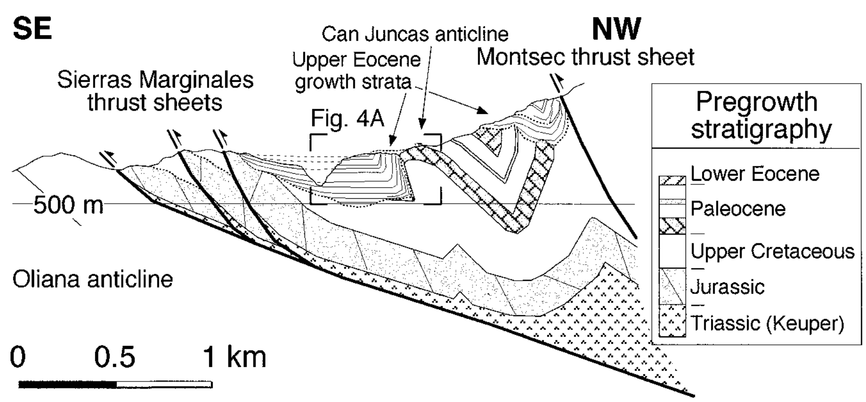

Figure 3. Regional cross section showing imbricate system of thrusts and folds above backlimb of Oliana anticline. Growth strata are linked to Can Juncas detachment anticline. Shaded units in pregrowth stratigraphy are competent layers.

The deformation path of the forelimb has been broken into horizontal and vertical components by tracking the motion of material points near the top of the forelimb (Fig. 4).

Overall, during 0.7 m.y., growth strata accumulated at a mean rate of ~0.16 mm/yr, as the forelimb rotated at a mean rate of ~1.3°/10^4 yr. In contrast to long-term rates, short-term rates (at the scale of single magnetic chrons) provide more insight on the interplay among variables that control the fold shape and patterns of growth strata. Although sedimentation rates were slow prior to 35.37 Ma (Fig. 4), they remained faster than the rate of forelimb uplift and resulted in onlap during early fold growth. Between 35.37 and 34.96 Ma, accumulation accelerated to ~0.16 mm/yr. However, because this rate is less than the vertical uplift rate (0.22 mm/yr), growth strata show offlap geometries and gentle thinning toward the crest of

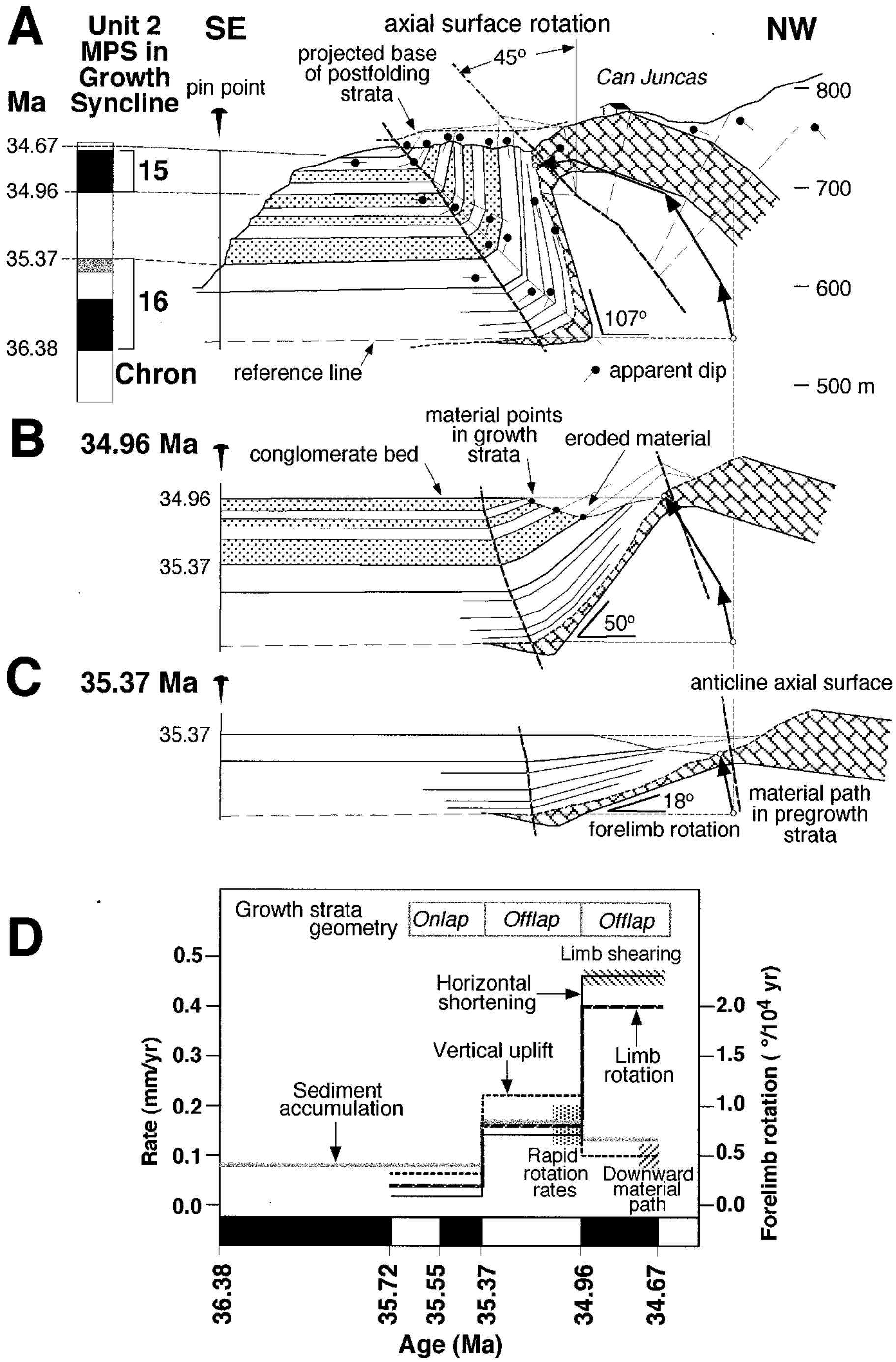

Figure 4. A: Detailed cross section of growth syncline at Can Juncas showing position of magnetostratigraphy (Burbank and Vergés, 1994). Prior to 36.4 Ma, growth strata filled paleovalley, and are not involved in unfolding. B: Unfolded geometry with strata younger than 34.96 Ma removed. For this and subsequent stages, total forelimb rotation and incremental movement of material points are shown. Positions of both synclinal and anticlinal axial surfaces are depicted. C: Unfolded geometry at 35.37 Ma. D: Mean chron-length rates of horizontal and vertical translation, limb rotation, and sediment accumulation during fold growth. Instantaneous rate changes at chron boundaries are not geologically meaningful. Ratios of vertical uplift to accumulation define intervals of onlap and offlap.

the anticline. Coevally, the forelimb steepened at a rate of ~0.8°/10^4 yr, and the fold achieved ~85% of its maximum height (Fig. 4B). Subsequently, from 34.96 to 34.67 Ma, accumulation rates dropped to ~0.13 mm/yr, whereas forelimb rotation increased almost 2.5 fold to ~2.0°/10^4 yr (Fig. 4B). During this stage, the uplift rate of the material points in growth strata at 34.96 Ma exceeded both the accumulation rate and the uplift rate of the material point in pregrowth strata. When combined with a rapid rate of horizontal shortening (~0.46 mm/yr), pronounced offlap developed. Although the extent to which layer-parallel slip contributes to the total shortening is difficult to quantify from field relations, some such slip is implied by our restorations, specifically in the lower stratal units (Fig. 4B).

DISCUSSION

Because both kinematics and structural geometry should be used to assess the validity of a cross section (Geiser, 1988), unfolding provides a useful constraint on the geometrical evolution of a fold and a check on the viability of an interpretation. Unfolding of dated growth strata reveals a detailed history of fold kinematics and changes in variables (rates of uplift, horizontal displacement, and limb rotation), which, along with rates of sediment accumulation and periods of erosion, affect the internal organization of the growth strata. The resultant geometric restorations can be compared with predicted geometries of published folding models. Our restorations at Can Juncas yield three critical fold-evolution observations (Fig. 4). First, the syncline axial surface changes its orientation through time, resulting in a broad hinge region. Axial surfaces of the present-day section are localized in this hinge region. Second, the forelimb rotates to a steeper dip toward the syncline with time. Third, the fold exhibits variable rates of crestal uplift and limb rotation during growth.

Delineation of the axial surfaces at each step helps define the growth and amplification of the fold. The fold grows and the forelimb rotates because the horizontal separation of the axial surfaces decreases with time, the axial surfaces concurrently rotate from a steeper to a shallower inclination, and the length of the forelimb does not change during folding (Fig. 4). Through time, the resultant deformational path of material points in the forelimb is forward and upward with respect to the syncline, until the forelimb is vertical. Subsequently, the path of these material points is forward and slightly downward (overturned limb).

Although the Can Juncas fold shows a superposition of axial surfaces within the hinge regions of the fold, other detachment folds in the Ebro region show pregrowth and growth strata passing forward through the anticlinal axial surface, such that crestal segments become incorporated into a lengthening forelimb (Millán et al., 1994). Whether axial surfaces have been fixed or active is often not easily discerned from a preserved fold geometry. Past changes in the orientation and position of such surfaces, however, can be defined through sequential unfolding of growth strata.

Given the time and geometric control at the Can Juncas anticline, rates of limb rotation, horizontal and vertical displacement, and sediment accumulation can be decoupled and independently compared (Fig. 4). Throughout growth, rates of limb rotation increase due to changes in the ratio of horizontal to vertical displacement. Whereas the rate of uplift is greater than horizontal shortening during the initial phases of folding (until the forelimb has attained 50° dip), horizontal displacement rates equal and subsequently exceed uplift after 34.96 Ma, resulting in shearing of the forelimb of the anticline. The growth-strata geometry is not completely defined, however, simply by comparison of rates of uplift and accumulation. Increased rates of limb rotation, driven by an acceleration of horizontal displacement and coupled with offlap, result in a strong angular discordance within the youngest growth strata (Fig. 4, A and B). Although the limb rotation rates we have documented are chron-length averages, pronounced tapering of several individual beds suggests that limb rotation rates vary on shorter time scales.

The evolving shape and related deformation rates of the Can Juncas fold can be compared with simple geometrical folding models which allow for increasing limb dips during growth. Models of symmetric chevron (Ramsay, 1974), sinusoidal (Rockwell et al., 1988), and detachment folds (Hardy and Poblet, 1994) predict that with a constant rate of horizontal shortening, high initial rates of uplift decay rapidly. In contrast, the rate of uplift at Can Juncas does not decrease with time because the rate of horizontal shortening accelerates. Similar to the model predictions, however, constant rates of uplift at Can Juncas can only be sustained by increasing rates of shortening through time. In the face of steady accumulation, these fold models each predict stratigraphic offlap, followed by onlap. Onlap geometries dominate the early folding at Can Juncas, and thus we interpret lower rates of vertical uplift for this time interval.

Rates of forelimb rotation are dependent on the geometry of folding, rates of shortening, and the wavelength of the growing fold. Fold wavelength is largely a function of the thickness of pregrowth strata. Comparable limb rotation rates would be expected only if the rates of shortening were scaled to variations in the pregrowth strata thickness and fold wavelength.

The hinge of the detachment fold at Can Juncas separates pregrowth strata of normal thickness from contiguous strata that had been thinned by erosion prior to the folding described here (Fig. 4). It might thus appear that this is not a particularly representative example of detachment folding, due to atypical initial conditions. It is likely, however, that the axes of folds are commonly positioned by differential thicknesses of pregrowth strata, because heterogeneities may localize strain.

CONCLUSIONS

Geometric models for fold development (Suppe, 1983; Suppe and Medwedeff, 1990) have served to focus attention on and to provide testable hypotheses for the kinematics and sequential growth of folds. Similarly, geometries of growth strata are predicted to record sensitively the evolving shape of the forelimb and backlimb of a fold. Given this prediction, interpretations of seismically imaged growth strata have been used to illustrate some folding models (Suppe et al., 1992). Neither the steep forelimb dips at Can Juncas anticline nor a fold of its scale, however, would be clearly imaged by typical seismic data. Yet, despite its small scale, the high-quality exposure and precise dating of the growth strata at Can Juncas provide powerful tools for examination of fold development through time. Whereas forward models *predict* fold evolution, unfolding of growth strata *reconstructs* incremental fold evolution. Furthermore, unfolding permits calculation of rates of deformation which, when combined with rates of deposition, emphasize the interactions among variable rates that determine the geometry of an evolving fold and related growth strata. Application of this methodology to other folds with associated growth strata should result in a more complete description and understanding of natural folding paths.

ACKNOWLEDGMENTS

Supported by the Subprograma Perfeccionamiento de Doctores and Dirección General de Investigación Científica y Técnica (grants PB91-0252 and PB91-0805 to Vergés), the National Science Foundation (grants EAR-9018951 and EAR-9304863 to Burbank), the Petroleum Research Fund of the American Chemical Society (grants PRF-17625 and PRF-23881 to Burbank), and the American Association of Petroleum Geologists, the Geological Society of America, and Sigma Xi (grants to Meigs). We thank M. López-Blanco for field assistance, and R. Allmendinger, J. Suppe, G. Axen, and two anonymous reviewers for constructive reviews.

REFERENCES CITED

Burbank, D. W., and Vergés, J., 1994, Reconstruction of topography and related depositional systems during active thrusting: Journal of Geophysical Research, v. 99, p. 20,281–20,297.

Burbank, D. W., Vergés, J., Muñoz, J. A., and Bentham, P. A., 1992, Coeval hindward- and forward-imbricating thrusting in the central southern Pyrenees: Timing and rates of shortening and deposition: Geological Society of America Bulletin, v. 104, p. 1–18.

Fischer, M. P., Woodward, N. B., and Mitchell, M. M., 1992, The kinematics of break-thrust folds: Journal of Structural Geology, v. 14, p. 451–460.

Geiser, P. A., 1988, The role of kinematics in the construction and analysis of geological cross sections in deformed terranes, *in* Mitra, G., and Wojtal, S., eds., Geometries and mechanisms of thrusting with special reference to the Appalachians: Geological Society of America Special Paper 222, p. 47–76.

Hardy, S., and Poblet, J., 1994, Geometric and numerical model of progressive limb rotation in detachment folds: Geology, v. 22, p. 371–374.

Jamison, W. R., 1987, Geometric analysis of fold development in overthrust terranes: Journal of Structural Geology, v. 9, p. 207–219.

Medwedeff, D. A., 1992, Geometry and kinematics of an active, laterally propagating wedge thrust, Wheeler Ridge, California, *in* Mitra, S., and Fisher, G. W., eds., Structural geology of fold and thrust belts: Baltimore, Maryland, Johns Hopkins University Press, p. 3–28.

Millán, H., Aurell, M., and Melendez, A., 1994, Synchronous detachment folds and coeval sedimentation in the Prepyrenean External Sierras (Spain): A case study for a tectonic origin of sequences and system tracts: Sedimentology, v. 41, p. 1001–1024.

Ramsay, J. G., 1974, Development of chevron folds: Geological Society of America Bulletin, v. 85, p. 1741–1754.

Riba, O., 1976, Syntectonic unconformities of the Alto Cardener, Spanish Pyrenees: A genetic interpretation: Sedimentary Geology, v. 15, p. 213–233.

Rockwell, T. K., Keller, E. A., and Dembroff, G. R., 1988, Quaternary rate of folding of the Ventura Avenue anticline, western Transverse Ranges, southern California: Geological Society of America Bulletin, v. 100, p. 850–858.

Shaw, J. H., and Suppe, J., 1994, Active faulting and growth folding in the eastern Santa Barbara Channel, California: Geological Society of America Bulletin, v. 106, p. 607–626.

Suppe, J., 1983, Geometry and kinematics of fault bend folding: American Journal of Science, v. 283, p. 648–721.

Suppe, J., and Medwedeff, D. A., 1990, Geometry and kinematics of fault-propagation folding: Eclogae Geologicae Helvetiae, v. 83, p. 409–454.

Suppe, J. S., Chou, G. T., and Hook, S. C., 1992, Rates of folding and faulting determined from growth strata, *in* McClay, K. R., ed., Thrust tectonics: London, Chapman and Hall, p. 105–122.

Vergés, J., 1993, Estudi geològic del vessant sud del Pirineu oriental i central. Evolució cinemàtica en 3D [Ph.D. thesis]: Barcelona, University of Barcelona, 203 p.

Vergés, J., and Muñoz, J. A., 1990, Thrust sequences in the southern central Pyrenees: Société géologique de France, Bulletin, v. 8, p. 399–405.

Manuscript received April 21, 1995
Revised manuscript received October 12, 1995
Manuscript accepted October 23, 1995